Journal of the European Ceramic Society **13** (1994) 395–401

Subeutectoid Precipitate Growth Activation Energies in Mg-PSZ

Charles S. Montross*

Electron Microscope Center and Department of Mining and Metallurgical Engineering, University of Queensland, Queensland, Australia 4072

(Received 23 June 1993; revised version received 1 November 1993; accepted 14 December 1993)

Abstract

The activation energy for lengthwise and widthwise precipitate growth in the subeutectoid region of Mg-PSZ was measured. The Arrhenius plot for both lengthwise and widthwise growth exhibited a two-slope behavior. The change in slope occurred at approximately the boundary between the tetragonal + MgO and the monoclinic + MgO two phase regions. The activation energies for both lengthwise and widthwise growth in the monoclinic + MgO two-phase region corresponded to the activation energy for Mg–Zr ion bulk or grain boundary interdiffusion. The higher activation energies for the tetragonal + MgO two-phase region are hypothesized to be due to interface controlled growth where the interface mobility is significantly less than the cation interdiffusion.

Die Aktivierungsenergie des Wachstums in Längs- und Querorientierung von Auscheidungen im untereutektoiden Bereich von Mg-PSZ wurde bestimmt. Die Arrheniuskurve für die beiden Wachstumsrichtungen zeigte ein Zweisteigungsverhalten Die Änderung der Steigung ergab sich ungefähr an der Grenze zwischen dem tetragonalen + MgO und dem monoklinen + MgO Phasengebiet. Die Aktivierungsenergie der beiden Wachstumsrichtungen im monoklinen + MgO Zweiphasengebiet entspricht der Aktivierungsenergie der Korngrenzendiffusion von Mg–Zr-Ionen im Probeninneren. Die höhere Aktivierungsenergie im tetragonalen + MgO Zweiphasengebiet ist vermutlich auf grenzflächenkontrolliertes Wachstum zurückzuführen, wobei die Mobilität der Grenzfläche bedeutend geringer ist als die Kationendiffusion.

On a mesuré l'énergie d'activation de la croissance de précipités, en largeur et en longueur, dans la région souseutectoïde de Mg-PSZ. Les traces d'Arrhenius pour la croissance en longueur ou en largeur présentent deux pentes caractéristiques. Le changement de pente se produit approximativement à la limite des domaines biphasés tétragonal + MgC) et monoclinique + MgO. Dans le domaine biphasé monoclinique + MgO, les énergies d'activation correspondent à l'énergie d'activation de l'ion Mg–Zr pour l'interdiffusion en volume ou aux joints de grains. Les énergies d'activation, plus élevées, du domaine biphasé tétragonal + MgO pourraient être dues à une croissance contrôlée par l'interface où la mobilité de l'interface serait très inférieure à la vitesse d'interdiffusion du cation.

1 Introduction

Research and development of partially stabilized zirconias has led to the industrial production and application of these various materials. Aspects of phase equilibria, crystallography, critical grain and precipitate size, and the resulting properties have been investigated and reported.[1] When zirconia is alloyed with magnesia and properly heat treated, a transformation toughened ceramic can result. For Mg-PSZ, the optimum temperature range for precipitating transformable tetragonal precipitates has been found to be the subeutectoid region.[2] More recent work has identified the critical precipitate size for optimum transformable tetragonal phase content and for optimum fracture toughness.[3]

Important parameters for future technological development of zirconia alloys are the activation energy for grain growth and precipitation and the growth of the various phases related to diffusion and ionic conduction of the relevant ions. The activation energy for diffusion and grain growth is useful for understanding the sintering of components and for creep behavior in high tempera-

* Present address: National Institute for Materials and Chemical Research, Tsukuba Research Center, 1-1 Higashi, Tsukuba, Ibaraki 305 Japan.

Journal of the European Ceramic Society 0955-2219/94/$7.00

ture applications. The activation energy for ionic conduction is important for various electrolyte applications while the activation energy for precipitate growth is important for controlling properties and size of metastable tetragonal phases.

Some early work on zirconia alloys involved calcia stabilized zirconia where Tien & Subbarao[4] and Rhodes & Carter[5] presented the activation energy for grain growth and for the diffusion of the anions and cations. More recently, the problem of silica and its affect on grain boundary migration in yttria–zirconia alloys,[6–8] (magnesia, calcia)–zirconia alloy[9] and ceria–zirconia alloys[10] was investigated. However, activation energies for the grain boundary migration were not presented.

Sintering and grain growth for yttria stabilized tetragonal and cubic zirconia were analyzed by Lee & Chen.[11] The activation energy of grain growth was reported as 105 kJ/mol for tetragonal zirconia and 69 kJ/mol for cubic zirconia. For the tetragonal case, the activation for grain growth correlated to the activation energy for self diffusion of the yttria ions in a cubic lattice.[12] The activation energy of 70 kJ/mol for grain growth in cubic zirconia was attributed by them to the activation energy for boundary diffusivity in yttria stabilized zirconia.

Hwang & Chen[13] further analyzed the grain growth kinetics of ceria and yttria tetragonal zirconia polycrystals (TZP) and the effect of doping by various cations. Grain size control of TZP ceramics is critical for controlling the resulting properties. Using the concept of space charge and electroneutrality of an ionic crystal, additions of cationic dopants may be used to control the grain growth, possibly by solute drag on the grain boundaries. They found that doping 12 mol.% ceria TZP with 1 mol.% alkali earths, the activation energy increased from 393 kJ/mol for undoped to 517 kJ/mol and 536 kJ/mol for MgO and CaO respectively. For 2 mol.% yttria TZP, the dopants segregated to the grain boundaries. In two other TZPs, In and Sc, the stabilizers also segregated to the grain boundaries.

With respect to Mg-PSZ, some work has been done on the grain boundary microstructure by Drennan & Hannink.[14] Silica is known to improve the sinterability and densification of Mg-PSZ, but at the expense of properties. Drennan & Hannink analyzed how additions of SrO improved the grain boundary such as by the gettering of the SiO_2 into the intergranular triple point junctions. Work on Mg-PSZ was expanded by Drennan & Swain[15] to include its sintering behavior. The density versus temperature was measured and the grain boundary microstructure was analyzed. In the work by Drennan & Hannink[14] and Drennan & Swain,[15] the activation energy for grain growth or sintering was not measured.

Precipitation in partially stabilized zirconias was investigated by Kim *et al.*[16] for the system (6 mol.% MgO, 4 mol.% CaO)-PSZ. The (MgO–CaO)-PSZ was aged at 1450°C for times up to 120 h. Intragranular precipitation occurred and the grain boundaries rapidly migrated. The grain boundary migration left behind large precipitates in a Ca-enriched precipitate-free cubic phase. The cause for this behavior was ascribed to coherency strain of the dopant cations at the grain–glassy grain boundary interface. No activation energy for grain or precipitate growth nor growth exponent for the precipitate free zone or for precipitate growth was presented.

For the MgO zirconia alloys, activation energies for both grain growth and precipitate growth are important but have not been noted in the literature. Precipitate growth activation energies are more important, since control of the precipitate behavior is critical for controlling the properties. The purpose of this research is to measure the activation energy for both lengthwise and widthwise precipitate growth. The subeutectoid region of the $MgO–ZrO_2$ phase diagram was investigated, since this is the region for optimum properties.[17]. The results were related to the phase equilibria of the $MgO–ZrO_2$ system and to existing knowledge of ionic conduction and activation energies.

2 Experimental Procedure

The 9·5 mol.% MgO–90·5 mol.% ZrO_2 Mg-PSZ composition was fabricated using high purity ZrO_2 (Z-Tech SF-Super Zirconia powder, Melbourne, Australia; SiO_2 < 80ppm) and MgO powders, sintered at 1700°C for 2 h and rapidly cooled to the required heat treatment temperatures.[3] The heating/sintering schedule is similar to that used commercially, resulting in a cubic solid solution with a grain size of approximately 30–40 μm. The effect of starting microstructure on precipitation behavior was not investigated.

The isothermal heat treatment temperatures investigated were 1400, 1380, 1320, 1260, 1200 and 1100°C. The times at these temperatures ranged from 0·25 at 1400°C to 20 h at 1100°C. The samples were ground then polished through 1 μm diamond grit. Polished samples were etched in concentrated 40 wt % HF acid for approximately 1·5 min. This method was used, since the high purity Mg-PSZ was very resistant to chemical attack and etching. After polishing and etching, the samples were carbon coated and prepared for

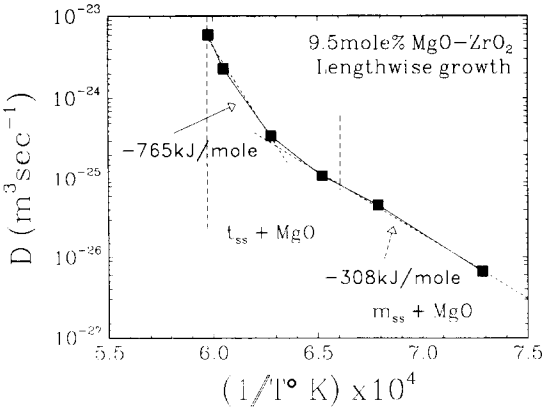

Fig. 1. Arrhenius plot for lengthwise growth of precipitates in Mg-PSZ. [length^3/time] versus 1/T°K. The phase lines are according to Grain.[20]

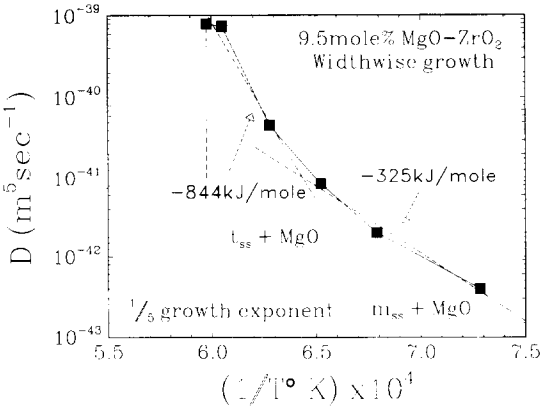

Fig. 2. Arrhenius plot for widthwise growth of precipitates in Mg-PSZ. [width^5/time] versus 1/T°K. The phase lines are according to Grain.[20]

analysis by scanning electron microscope (SEM). Typical regions were identified and electron micrographs were taken. Prints of these micrographs were enlarged and an average of 60 precipitates per temperature and time were measured for length and width.

3 Results

The length and width measurements were analyzed with respect to the following equation:

$$S^n - S_0^n = tAe \exp(-(E_a/RT))$$

where t is time, A is the pre-exponential, E_a is the activation energy, n is the growth exponent, and S_0 is the initial precipitate size. The initial precipitate size was assumed to be equal to zero in this analysis. For lengthwise growth, the growth exponent used for analysis was $n = 3$, which corresponds to volume diffusion controlled growth. For widthwise growth, a growth exponent of $n = 5$ was used, which corresponds to growth across low angle grain boundaries, boundary mismatch, or boundary misorientation. These two growth exponents were found to apply to precipitate growth in Mg-PSZ.[18]

In Table 1, the temperature, average precipitate (length)^3/time with its standard deviation, and the precipitate's (width)^5/time and its standard deviation are listed. In Fig. 1, (length)^3/time was plotted, without error bars, versus the inverse of temperature in degrees K. The plotted data shows a change in slope at approximately 1312°C, which is above the tetragonal + MgO and monoclinic + MgO phase boundary. Linear least squares analysis was used to calculate the two slopes. For the tetragonal + MgO region, the data points 1400, 1380 and 1320°C were used. For the monoclinic + MgO region, the data points 1260, 1200, and 1100°C were used. The activation energies and pre-exponentials are listed in Table 2.

In Fig. 2, (width)^5/time is plotted versus the inverse of temperature in degrees K. The plotted data also shows a change in slope at approximately 1281°C just above the phase boundary. As

Table 1. Temperature, precipitate's (length)^3/time, and its standard deviation, and (width)^5/time and its standard deviation

Temperature (°C)	*(length)^3/time (m^3/s)*	*Standard deviation ± (m^3/s)*	*(width)^5/time (m^5/s)*	*Standard deviation ± (m^5/s)*
1400	5.955×10^{-24}	0.168×10^{-24}	7.944×10^{-40}	0.082×10^{-42}
1380	2.276×10^{-24}	0.022×10^{-24}	7.329×10^{-40}	0.005×10^{-42}
1320	3.461×10^{-25}	0.074×10^{-25}	4.581×10^{-41}	0.447×10^{-43}
1260	1.082×10^{-25}	0.012×10^{-25}	8.308×10^{-42}	0.108×10^{-44}
1200	4.563×10^{-26}	0.012×10^{-26}	1.993×10^{-42}	0.009×10^{-44}
1100	6.620×10^{-27}	0.006×10^{-27}	3.986×10^{-43}	0.008×10^{-45}

Table 2. Activation energies and pre-exponentials for precipitate growth in Mg-PSZ

Precipitate measurement	*Temperature range (°C)*	*ln (pre-exponential) (ln (A))*	*Activation energy (E_a kJ/mol)*
Lengthwise	1400–1320	+1.388 ± 0.21	−765 ± 79
Lengthwise	1260–1100	−33.275 ± 0.09	−308 ± 14
Widthwise	1400–1320	−29.055 ± 0.48	−844 ± 180
Widthwise	1260–1100	−69.204 ± 0.29	−325 ± 45

for the lengthwise growth, linear least squares analysis was used for calculating the two slopes using the same temperatures.

4 Discussion

4.1 Relationship of results with ZrO_2–MgO phase equilibria

Grain[19] analyzed the phase equilibria in the ZrO_2–MgO system and reported a eutectoid composition of 13 mol.% MgO with the tetragonal$_{ss}$ + MgO and monoclinic$_{ss}$ + MgO phase boundary at 1240°C. Echigoya *et al.*[20] analyzed the decomposition of hypoeutectoid Mg-PSZ from 1000 to 1300°C. They found that the tetragonal + MgO and monoclinic + MgO phase boundary was approximately 1185 ± 45°C with the eutectoid composition at 11 mol.% MgO. In the review and re-evaluations of phase equilibria in the three zirconia systems, Stubican[21] noted the phase diagram presented by Grain as being currently accepted. More recent work by Duran *et al.*[22] also place the phase boundary at a lower temperature, at approximately 1120°C. In this research, the change in slope at approximately 1312°C occurs for the lengthwise growth of the precipitates. The change in slope for the widthwise growth of precipitates, at approximately 1281°C, will not be closely considered due to the high standard deviation for the upper widthwise growth pre-exponential. These results support the higher phase transition temperature presented by Grain for a phase boundary at 1240°C. Future research should investigate differing compositions with three to four temperatures analyzed per phase region to more accurately identify the phase boundary.

4.2 Precipitation behavior and activation energies

4.2.1 Literature review

The precipitates in Mg-PSZ can be described as ellipsoidal, like disks, where in cross-section at the edge of the disk, the interface is coherent and the lattice parameters between the cubic and tetragonal phase match, $a_{cubic} = a_{tetrag}$.[23] Where the interface is coherent, growth is controlled by volume diffusion. On the broad side of the precipitate, the interface is semi- or incoherent where the c_{tetrag} axis mismatches the a_{cubic} axis. The growth on this interface is controlled by the boundary mismatch and the short circuit diffusion along low angle boundaries. In the tetragonal + MgO two-phase region, the growth exponent is known,[18] where for lengthwise growth, it is 1/3, and for widthwise growth, it is 1/5.

When the precipitate nucleus forms, MgO is expelled or exsolves from the precipitate. As it grows, MgO is expelled from the boundary region into the cubic matrix, while the zirconia diffuses in the opposite direction across the boundary into the precipitate. The segregation of the MgO from the precipitate has been noted from the phase equilibria studies of Grain[19] and Stubican.[21] Grain and Stubican reported that the solubility of MgO in the tetragonal precipitates is less than 1 mol.%. Echigoya *et al.*[20] reported that there was no MgO in the zirconia precipitates when aged at 1100°C. The predominant defect within the precipitate itself is assumed to be anion Frenkels, interstitial oxygen ions and oxygen ion vacancies, based on the work by Douglas & Wagner[24] on pure monoclinic zirconia.

The concentration of MgO in the matrix increases with time to form MgO pipes and to concentrate in the cubic center of the grain.[25,26] At the boundary of the precipitate, the MgO concentration was found to be enriched up to 28 mol.%.[27] Hannink[28] and Farmer *et al.*[26] also found that as the MgO concentration increases in the cubic phase, the rate of decomposition increases.

The diffusion of oxygen ions in magnesia stabilized zirconia was analyzed by Ando *et al.*[29] for concentrations of 12 to 16 mol.% MgO. As shown in Fig. 3 for 12 mol.% MgO, the activation energy increases with decreasing temperature and is tied to the phase equilibria of the system. Based on their data points, the activation energy for the tetragonal$_{ss}$ + MgO phase region is −117 kJ/mol which increases to −195 kJ/mol for the monoclinic$_{ss}$ + MgO phase region. They also found that as the concentration of MgO increases, the activation energy also increases. Similar behavior was found by Badwal[30] for yttria stabilized zirconia where decreasing temperature or increasing stabilizer content results in increasing activation energy. Douglas & Wagner[24] also measured the activation energy for oxygen diffusion for reduced pure monoclinic zirconia. They found that between 450 and

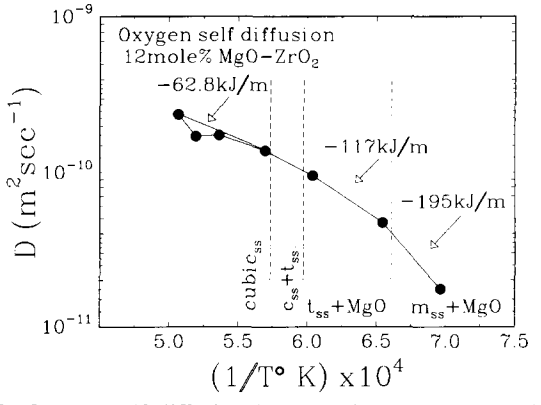

Fig. 3. Oxygen self diffusion in 12 mol.% MgO–ZrO_2 showing the effect of phase boundaries on activation energy. From K. Ando *et al.*[30]

900°C for $ZrO_{1.994}$, the activation energy for oxygen diffusion was −277 kJ/mol.

Wen *et al.*[31] measured the oxygen ionic conductivity versus temperature and magnesia content from 6 to 12 mol.%. They found that the ionic conductivity increased with increasing magnesia content from 6 to 8 mol.% then decreased. However no activation energies were given. This behavior is similar to that exhibited for yttria stabilized zirconia which has a peak in ionic conductivity at approximately 8 mol.% yttria.[30]

A summary of the results for oxygen ionic conductivity is that with decreasing temperature the activation energy increases. Additionally, increasing magnesia content results in increasing activation energy as measured by Ando *et al.* However, there is also a peak in conductivity, as noted by Wen *et al.*

Magnesia ion diffusivity in zirconia has been measured by Sakka *et al.*[32] by evaporation of the magnesia at temperatures of 1800 to 2100°C. They found that the evaporation kinetics were enhanced by the presence of grain boundaries and controlled by cationic interdiffusion. The cationic interdiffusion in MgO stabilized zirconia was measured by Oishi *et al.*[33] between 1600 and 2000°C. For lattice interdiffusion, the activation energy was −293 kJ/mol, while for grain boundary interdiffusion the activation energy was −297 kJ/mol.

The individual diffusion activation energies have been reported by Sakka *et al.*[34] as being −285 kJ/mol for magnesia and −381kJ/mol for zirconia in magnesia stabilized zirconia. They found that the cation interdiffusion was controlled primarily by the diffusion of the faster cation. The contribution by the high diffusivity of the oxygen ion was considered small by them.

A theoretical analysis of the point defect activation energies in cubic zirconias for 1250°C was presented by Mackrodt & Woodrow.[35] The heats of solution listed by them for magnesia are H_0 = 300kJ/mol and H_A = 154 kJ/mol, where H_0 is when there is no association between the impurity and vacancy defects and where H_A is when the impurity ion completely associates with the defect. The migration energies are: anion vacancies = −63kJ/mol; cation vacancies = −826 kJ/mol; neutral vacancy complexes = −846 kJ/mol; and anion vacancies in the presence of impurity MgZr + 2 ions = −98 kJ/mol.

4.2.2 Discussion

The activation energies in the monoclinic + MgO two-phase region corresponds most closely to the Mg–Zr lattice (–293 kJ/mol) and grain boundary (–297 kJ/mol) interdiffusion activation energies reported by Oishi *et al.*[33] Differences between the values reported by Oishi *et al.* and the values measured in this research for lengthwise (−308 kJ/mol) and widthwise (−325 kJ/mol) growth, can be accounted for by consideration of changes in activation energy with changing temperature regimes, 1600–2000°C by Oishi *et al.* and 1400–1100°C in this work. This effect was found by Ando *et al.*[29] for oxygen diffusivity in Mg-PSZ. In the tetragonal + MgO two-phase region, the higher activation energies do not correspond to any reported single mechanism.

Changes in activation energy cannot be attributed to grain boundary drag due to the formation of the δ-phase at the precipitate–matrix boundary. Farmer *et al.*[26] found that at 1100°C, the dominant decomposition mechanism is the formation of monoclinic ZrO_2 at the grain boundaries which propagates into the grain along with pipes of MgO. Samples with increasing MgO content resulted in an increasing rate of decomposition. Their Fig. 3 shows $Mg_2Zr_5O_{12}$, precipitates surrounding a tetragonal ZrO_2, precipitate. To precipitate the δ phase, a special heat treatment was required. This consisted of solution treating in the cubic solid solution region at 1800°C, cooling to 800°C for 1 h, followed by precipitation at 1100°C for 10 h.

Interface migration and growth of precipitates can be controlled by the interface mobilities.[36,37] Interfaces with high mobilities typically have high interface energies, such as incoherent precipitates in metallurgical systems. High mobility interfaces move as fast as diffusion of the rate-controlling species allows and growth is considered to be diffusion controlled. Low mobility interfaces typically have low interface energies and are typically coherent precipitates in metallurgical systems. Larger chemical potential differences are then required to drive the interface and growth is considered to be either mixed or interface controlled. The activation energy would then be higher than for diffusion controlled growth.

In the Mg-PSZ system, surface and strain energies of the metastable precipitates can be considered to have an effect. At non-equilibrium conditions in the monoclinic + MgO two-phase region, a metastable tetragonal phase is precipitating in a cubic matrix. The strain and surface energies and the thermodynamic driving force for transformation of the metastable tetragonal precipitate affect the interface, raising the total interface energy and thereby increasing its mobility. The interface becomes diffusion controlled and as the experimental results indicate, the measured activation energy matches that for Mg–Zr interdiffusion.

In the tetragonal + MgO two-phase region, stable tetragonal precipitates form in a cubic matrix.

The tetragonal precipitates are thermodynamically stable, since they are growing above the tetragonal–monoclinic transition temperature. In the production of Mg-PSZ, precipitates do not become metastable until cooled below this transition temperature.[1] Therefore, the interface energies can be considered lower than in the monoclinic + MgO two-phase region. Due to the lower interface energies, the mobility is lower and growth becomes interface-controlled. Interface controlled growth would have higher activation energies than for Mg–Zr interdiffusion.

5 Conclusions

Based on the present results, the following conclusions can be reached.

(a) The change in slope of the activation energies corresponds to the phase boundary between the tetragonal + MgO two-phase region and the monoclinic + MgO two-phase region. The temperature at which the change of slope occurs, 1312°C, supports the higher phase boundary temperature for the MgO—ZrO_2 phase diagram presented by Grain.

(b) The activation energy for both lengthwise and widthwise precipitate growth in the monoclinic + MgO two phase region corresponds to the activation energy for Mg–Zr lattice and grain boundary interdiffusion.

(c) The activation energy for both lengthwise and widthwise precipitate growth in the tetragonal + MgO two-phase region does not correspond to any single diffusion mechanism. It is theorized that since a thermodynamically stable tetragonal phase is precipitating in the tetragonal + MgO two-phase region, the interface energies are lower than in the monoclinic + MgO two-phase region. The resulting precipitate growth is interface controlled with a higher activation energy than for diffusion.

Acknowledgements

The author would like to express his appreciation for the interest and constructive comments of Dr Bart van Hassel and Dr Harumi Yokokawa. He would also like to express his appreciation for the assistance and support of the research staff at the Electron Microscope Center and at the Department of Mining and Metallurgical Engineering, University of Queensland, Australia, and to express his appreciation to the Australian Industrial Research and Development Board for the funding for this research through grant number 15010 via the Electron Microscope Center and the Department of Mining and Metallurgical Engineering.

References

1. Green, D. J., Hannink, R. H. J. & Swain, M. V., *Transformation Toughening of Ceramics*. CRC Press, Boca Raton, FL, 1989.
2. Hughan, R. R. & Hannink, R. H. J., Precipitation during controlled cooling of magnesia-partially-stabilized zirconia. *J. Am. Ceram. Soc.*, **69** (1986) 556–63.
3. Montross, C. S., Relationships of tetragonal precipitate statistics with bulk properties in magnesia partially stabilized zirconia. *J. Eur. Ceram. Soc.*, **11** (1993) 471–80.
4. Tien, T. Y. & Subbarao, E. C., Grain growth in $Ca_{0.16}Zr_{0.84}O_{1.84}$. *J. Am. Ceram. Soc.*, **46** (1963) 489–92.
5. Rhodes, W. H. & Carter, R. E., Cationic self-diffusion in calcia-stabilized zirconia. *J. Am. Ceram. Soc.*, **49** (1966) 244–9.
6. Chaim, R., Rühle, M. & Heuer, A. H., Microstructural evolution in ZrO_2–12 wt% Y_2O_3 ceramics. *J. Am. Ceram. Soc.*, **68** (1985) 427–36.
7. Chaim, R., Heuer, A. H. & Brandon, D. G., Phase equilibria in ZrO_2–Y_2O_3 alloys by liquid film migration. *J. Am. Ceram. Soc.*, **69** (1986) 243–8.
8. Stoto, T., Nauer, M. & Carry, C., Influence of residual impurities on phase partitioning and grain growth processes of Y-TZP materials. *J. Am. Ceram. Soc.*, **74** (1991) 2615–21.
9. Butler, E. P. & Heuer, A. H., Grain boundary phase transformation during aging of a partially stabilized ZrO_2—a liquid phase analogue of diffusion induced grain-boundary migration (DIGM) (?). *J. Am. Ceram. Soc.*, **68** (1985) 197–202.
10. Schmid, H. K., Diffusion-Induced grain-boundary migration in ceria stabilized tetragonal zirconia polycrystals. *J. Am. Ceram. Soc.*, **74** (1991) 387–94.
11. Lee, I. G. & Chen, I-Wei, Sintering and grain growth in tetragonal and cubic zirconia. In *Sintering '87*, ed. S. Sōmiya, M. Shimada, M. Yoshimura & R. Watanabe. Elsevier Applied Science, Tokyo, 1988, pp. 340–5.
12. Oishi, Y., Ando, K. & Sakka, Y., Lattice and grain boundary diffusion coefficients of cations in stabilized zirconias. *Adv. Ceram.*, **7** (1983) 208–19.
13. Hwang, Shyh-Lung & Chen, I-Wei, Grain size control of tetragonal zirconia polycrystals using the space charge concept, *J. Am. Ceram. Soc.*, **73** (1990) 3269–77.
14. Drennan, J. & Hannink, R. H. J., Effect of SrO additions on the grain boundary microstructure and mechanical properties of magnesia-partially stabilized zirconia. *J. Am. Ceram. Soc.*, **69** (1986) 541–6.
15. Drennan, J. & Swain, M. V., Sintering of magnesia partially stabilised zirconia (Mg-PSZ). In *Sintering '87*, ed. S. Sōmiya, M. Shimada, M. Yoshimura & R. Watanabe. Elsevier Applied Science, Tokyo, 1988, pp. 1118–23.
16. Kim, J. J., Park, C., Kim, D. Y., Yoon, D. N. & Shapiro, A., Discontinuous coarsening of tetragonal precipitates in PSZ induced by differential coherency strain under applied stress. *J. Am. Ceram. Soc.*, **73** (1990) 3658–62.
17. Hughan, R. R. & Hannink, R. H. J., Precipitation during controlled cooling of magnesia-partially-stabilized zirconia. *J. Am. Ceram. Soc.*, **69** (1986) 556–63.
18. Montross, C. S., Tetragonal precipitates growth in Mg-PSZ. In *Proc International Cer. Conf. AustCeram90*, Perth, August 1990, ed. P. J. Darragh & R. J. Stead. pp. 772–7.

19. Grain, C. F., Phase relations in the ZrO_2–MgO system. *J. Am. Ceram. Soc.*, **50** (1967) 288–90.
20. Echigoya, J., Sasai, K. & Suto, H., Microstructural change of 11 mol.% MgO–ZrO_2 by aging. *Trans. Japan Inst. Metals*, **29** (1988) 561–9.
21. Stubican, V. S., Phase equilibria and metastabilities in the systems ZrO_2–MgO, ZrO_2–CaO, and ZrO_2–Y_2O_3. In *Advances in Ceramics*, Vol. 24, *Science and Technology of Zirconia*, III, Ed. S. Sōmiya, N. Yamamoto & H. Yanagida. The American Ceramic Society. Westerville, OH, 1988, pp. 71–81.
22. Duran, P., Rodriguez, J. M. & Recio, P., The ZrO_2-rich region of the ZrO_2–MgO System. *J. Mater. Sci.*, **26** (1991) 467–72.
23. Hannink, R. H. J., Growth morphology of the tetragonal phase in partially stabilized zirconia. *J. Mater. Sci.*, **13** (1978) 2487–96.
24. Douglas, D. L. & Wagner, C., The oxidation of oxygen deficient zirconia and its relationship to the oxidation of zirconia. *J. Electrochem. Soc.*, **113** (1966) 671–6.
25. Hay, S., Nairn, J. D. & StJohn, D. H., Secondary precipitate growth in Mg-PSZ. In *Proc. International Cer. Conf., AustCeram90*, Perth, August 1990, ed. P. J. Darragh & R. J. Stead. pp. 744–9.
26. Farmer, S. C., Mitchell, T. E. & Heuer, A. H., Diffusional decomposition of c-ZrO_2 in Mg-PSZ. In *Advances in Ceramics*, Vol. 12, *Science and Technology of ZrO_2 II*, ed. N. Claussen, M. Rühle & A. H. Heuer. The American Ceramic Society, Columbus, OH, 1984, pp. 152–63.
27. Hannink, R. H. J., Maher, D. M. & Cliff, G., MgO segregation in decomposed MgO–ZrO_2 alloys. *J. Aust. Ceram. Soc.*, **20** (1985) 38–41.
28. Hannink, R. H. J., Microstructural development of subeutectoid aged MgO–ZrO_2 alloys. *J. Mater. Sci.*, **18** (1983) 4457–70.
29. Ando, K., Oishi, Y., Koizumi, H. & Sakka, Y., Lattice defect and oxygen self diffusion in MgO-stabilized ZrO_2. *J. Mater. Sci. Lett.*, **4** (1985) 176–80.
30. Badwal, S. P. S., Zirconia-based solid electrolytes: microstructures, stability and ionic conductivity. *Solid State Ionics*, **52** (1992) 23–32.
31. Wen, Tinglian, Li, Ziaofei, Kuo, Chukun & Weppner, W., Conductivity in MgO-doped ZrO_2. *Solid State Ionics*, **18–19** (1986) 715–19.
32. Sakka, Y., Oishi, Y. & Ando, K., Enhancement of MgO evaporation from MgO-stabilized ZrO_2 by grain-boundary diffusion. *J. Am. Ceram. Soc.*, **69** (1986) 111–13.
33. Oishi, Y., Ando, K. & Sakka, Y., Lattice and grain-boundary diffusion coefficients of cations in stabilized zirconia. In *Additives and Interfaces in Electrical Ceramics, Advances in Ceramics*, Vol. 7, ed. M. F. Yan & A. H. Heuer. The American Ceramic Society Columbus, OH, 1983, pp. 208–19.
34. Sakka, Y., Oishi, Y. & Ando, K., Cation interdiffusion in polycrystalline fluorite MgO–ZrO_2 solid solutions. *Bull. Chem. Soc. Jpn*, **55** (1982) 420–2.
35. Mackrodt, W. C. & Woodrow, P. M., Theoretical estimates of point defect energies in cubic zirconia. *J. Am. Ceram. Soc.*, **69** (1986) 277–80.
36. Porter, D. A. & Easterling, K. E., *Phase Transformations in Metals and Alloys*, Van Nostrand Reinhold (UK) Co. Ltd, Berkshire, UK, 1981, pp. 176–80.
37. Hillert, M., Diffusion and interface control of reactions in alloys. *Met. Trans. A*, **6A** (1975) 5–19.